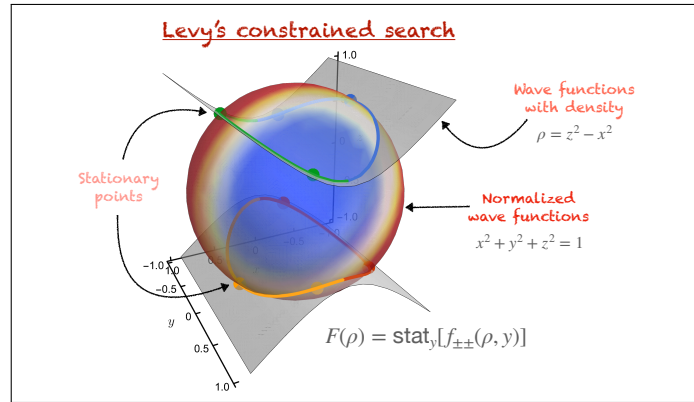


Exact Excited-State Functionals of the Asymmetric Hubbard Dimer

Sara Giarrusso^{1, a)} and Pierre-François Loos^{1, b)}

Laboratoire de Chimie et Physique Quantiques (UMR 5626), Université de Toulouse, CNRS, UPS, France

Abstract: The exact functionals associated with the (singlet) ground and the two singlet excited states of the asymmetric Hubbard dimer at half-filling are calculated using both Levy’s constrained search and Lieb’s convex formulation. While the ground-state functional is, as commonly known, a convex function with respect to the density, the functional associated with the doubly-excited state is found to be concave. Also, because the density-potential mapping associated with the first excited state is non-invertible, its “functional” is a partial, multi-valued function composed of one concave and one convex branch that correspond to two separate domains of values of the external potential. Remarkably, it is found that, although the one-to-one mapping between density and external potential may not apply (as in the case of the first excited state), each state-specific energy and corresponding universal functional are “functions” whose derivatives are each other’s inverse, just as in the ground state formalism. These findings offer insight into the challenges of developing state-specific excited-state density functionals for general applications in electronic structure theory.



Several decades after its foundation,¹ density-functional theory (DFT) still represents the main computational tool to perform quantum mechanical simulations of interest for pharmaceutical and technological applications.² Originally developed as a ground-state theory, it has been swiftly extended to calculate the lowest excited state of a given symmetry,^{3–7} thereby obtaining excitation energies from differences of self-consistent field (Δ SCF) calculations.

Notwithstanding the usefulness of such extension, for more general purposes, one usually relies on (linear-response) time-dependent (TD) DFT to describe excited states at the DFT level.^{8–12} TDDFT is an in-principle exact theory but, in practice, it relies on approximations for the exchange-correlation kernel. A fundamental source of error underlying virtually all its implementations is adiabaticity (neglecting memory effects), while another type of error comes from the particular choice of the exchange-correlation functional, similar to ground-state Kohn-Sham DFT.¹³ Within these approximations, TDDFT has seen important successes¹⁴ but is also plagued by well-known shortcomings, e.g., for the description of double excitations or charge-transfer processes.^{15–20}

Due to the relevance of these phenomena in photochemical applications or quantum-based technologies, alternative, time-independent theories have been developed. The most well-known is ensemble DFT (EDFT), based on an ensemble of equally-weighted²¹ or unequally-weighted^{22–24} densities, each coming from an individual quantum state rather than a pure-state density as in traditional DFT. In recent times, EDFT and related theories have undergone significant developments that are crucial to its advancement.^{25–49} However, it suffers from the disadvantages that, to treat a high-lying excited state, it is usually required to include all lower-lying states in the ensemble, and that the weight dependence of the exchange-correlation functional is hard to model. Another ensemble theory that has been receiving increasing attention and shares some of the problems of EDFT is w -ensemble one-body reduced density matrix functional theory.^{45–49}

Concerning pure excited states, orbital-optimized DFT,^{50–63} the extension to any excited state of the mentioned Δ SCF calculations, has been shown to be relatively successful for the calculation of classes of excitations where TDDFT typically fails,^{55,56} although its theoretical underpinning is still in progress.

From a theoretical perspective, state-specific density-functional formalisms have been developed.^{64–73} Some of these are complicated by the dependence of the functional

^{a)} Electronic mail: sgiarrusso@irsamc.ups-tlse.fr

^{b)} Electronic mail: loos@irsamc.ups-tlse.fr

on quantities other than the excited-state density and/or by the need for orthogonality constraints to inherit the variational character of the ground-state theory.⁷⁴

In his seminal work, Görling⁶⁷ proposes a *stationarity* rather than a *minimum* principle to treat excited states. Building on Görling’s work⁶⁹ and restricting the set of external potentials to Coulombic ones, Ayers *et al.* establish a one-to-one mapping between external potential and any of its associated stationary densities.^{70–72} For a general external potential, this one-to-one mapping may not hold true.^{50,75–77} However, none of these formalisms have revealed a fundamental dual relationship between excited-state energy and its corresponding state-specific functional similar to the one between the ground-state energy and the universal functional elucidated by Lieb.⁷⁸

In turn, the present Letter provides an explicit case in which such a fundamental dual relationship carries through for excited states. Adopting Görling’s stationarity principle⁶⁷ on Levy’s constrained search⁷⁹ and Lieb’s convex formulation,⁷⁸ we find for a simple model that, just as for the ground state, a given excited-state energy and its corresponding universal functional are functions whose derivatives are each other’s inverse functions, a property described as “the essence of DFT”.⁸⁰ Yet the “functional” associated with the first-excited state has some very peculiar mathematical properties.

Below, we first review the ground-state formalism. Consider the usual variational principle

$$E[v] = \min_{\Psi} \langle \Psi | \hat{H}_v | \Psi \rangle \quad (1)$$

where the minimization is performed over all normalized N -electron antisymmetrized wave functions Ψ and the electronic Hamiltonian

$$\hat{H}_v = \hat{T} + \hat{V}_{ee} + \sum_{i=1}^N v(\mathbf{r}_i) \quad (2)$$

is composed of the kinetic energy operator \hat{T} , the electron repulsion operator \hat{V}_{ee} , and the external potential contribution.

The minimization in Eq. (1) can be split in two steps

$$\begin{aligned} E[v] &= \min_{\rho} \min_{\Psi \rightsquigarrow \rho} \langle \Psi | \hat{H}_v | \Psi \rangle \\ &= \min_{\rho} \left\{ F[\rho] + \int v(\mathbf{r}) \rho(\mathbf{r}) d\mathbf{r} \right\} \end{aligned} \quad (3)$$

where in the second line we have introduced the Levy-Lieb or “universal” functional defined, via Levy’s constrained search,⁷⁹ as

$$F[\rho] = \min_{\Psi \rightsquigarrow \rho} \langle \Psi | \hat{H}_0 | \Psi \rangle = \langle \Psi[\rho] | \hat{H}_0 | \Psi[\rho] \rangle \quad (4)$$

Note that the Hohenberg-Kohn,¹ Levy-Lieb,^{78,79} or Lieb functional⁷⁸ differ in the density domain. We refer to any of them as the universal functional, although only the Lieb functional is properly convex in ρ .⁸⁰

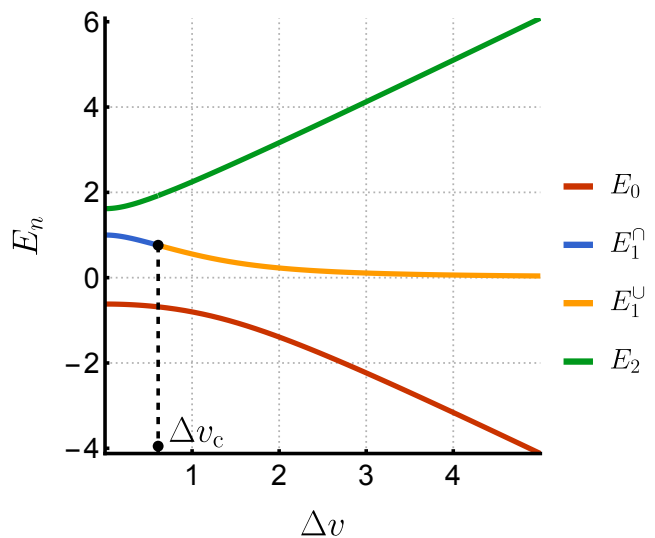


FIG. 1. E_0 , E_1 , and E_2 as functions of Δv for $t = 1/2$ and $U = 1$. Note that E is an even function of Δv . E_1 is concave for $\Delta v < \Delta v_c$ and becomes convex for larger Δv values.

The Legendre-Fenchel transform of Eq. (3) delivers $F[\rho]$ from the maximisation

$$F[\rho] = \max_v \left\{ E[v] - \int v(\mathbf{r}) \rho(\mathbf{r}) d\mathbf{r} \right\} \quad (5)$$

exemplifying the duality between the functional $E[v]$, concave in the external potential v , and $F[\rho]$, convex in the density ρ .⁷⁸ Although technically discontinuous, $F[\rho]$ is “almost differentiable”⁸⁰ in that it may be approximated to any accuracy by a differentiable regularized functional.⁸¹ Thus, assuming differentiability and carrying out the optimizations in Eqs. (3) and (5), one obtains

$$\frac{\delta F[\rho(\mathbf{r})]}{\delta \rho(\mathbf{r})} + v(\mathbf{r}) = 0 \quad (6a)$$

$$\frac{\delta E[v(\mathbf{r})]}{\delta v(\mathbf{r})} - \rho(\mathbf{r}) = 0 \quad (6b)$$

respectively.

We adopt the two-site Hubbard model at half-filling,^{31,82–91} whose Hamiltonian reads

$$\hat{H} = -t \sum_{\sigma=\uparrow,\downarrow} \left(a_{0\sigma}^\dagger a_{1\sigma} + \text{h.c.} \right) + U \sum_{i=0}^1 \hat{n}_{i\uparrow} \hat{n}_{i\downarrow} + \Delta v \frac{\hat{n}_1 - \hat{n}_0}{2} \quad (7)$$

where $t > 0$ is the hopping parameter, $U \geq 0$ is the on-site interaction parameter, $\hat{n}_{i\sigma} = a_{i\sigma}^\dagger a_{i\sigma}$ is the spin density operator on site i , $\hat{n}_i = \hat{n}_{i\uparrow} + \hat{n}_{i\downarrow}$ is the density operator on site i , and $\Delta v = v_1 - v_0$ (with $v_0 + v_1 = 0$) is the potential difference between the two sites.

Although simple, this model is able to describe the physics of partially-filled narrow band gaps^{82,83,85} and its two-site version has been used in the framework of site-occupation function theory to exemplify central concepts

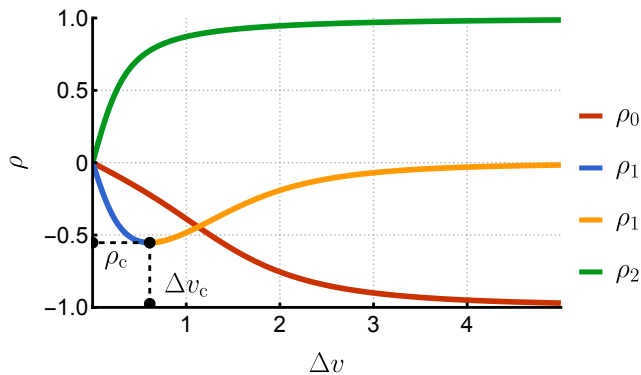


FIG. 2. ρ as a function of Δv for $t = 1/2$ and $U = 1$ for the ground-state (ρ_0), the singly-excited state (ρ_1), and the doubly-excited states (ρ_2). ρ_1 reaches a critical value, ρ_c , at Δv_c . Note that ρ is an odd function of Δv .

or test (new) density-functional methods by numerous authors.^{31,84,86-91}

It is noteworthy to mention that for lattice systems, even in the case of the ground-state functional, the Hohenberg-Kohn theorem does not hold universally. While a potential does exist, it is not always unique. This aspect was recently highlighted by Penz and van Leeuwen.⁹² However, in the context of linear Hubbard chains (like the one discussed in this paper where the chain is of length two), the uniqueness and thus the applicability of the Hohenberg-Kohn theorem is established by Theorem 17 in the aforementioned reference. This theorem provides a robust guarantee of uniqueness, ensuring that for linear Hubbard chains, there is a unique potential associated with a given density. Notably, the present study and Schönhammer and Gunnarsson's original work also support this.⁸⁴

At half filling ($N = 2$), we expand the Hamiltonian in the N -electron (spin-adapted) site basis $|0_\uparrow 0_\downarrow\rangle$, $(|0_\uparrow 1_\downarrow\rangle - |0_\downarrow 1_\uparrow\rangle)/\sqrt{2}$, and $|1_\uparrow 1_\downarrow\rangle$ to form the following Hamiltonian matrix

$$\mathbf{H} = \begin{pmatrix} U - \Delta v & -\sqrt{2}t & 0 \\ -\sqrt{2}t & 0 & -\sqrt{2}t \\ 0 & -\sqrt{2}t & U + \Delta v \end{pmatrix} \quad (8)$$

whose eigenvalues provide the singlet energies of the system. A generic singlet wave function can then be written as

$$|\Psi\rangle = x |0_\uparrow 0_\downarrow\rangle + y \frac{|0_\uparrow 1_\downarrow\rangle - |0_\downarrow 1_\uparrow\rangle}{\sqrt{2}} + z |1_\uparrow 1_\downarrow\rangle \quad (9)$$

with $-1 \leq x, y, z \leq 1$ and the normalization condition

$$x^2 + y^2 + z^2 = 1 \quad (10)$$

The energy is given by $E = T + V_{ee} + V$, with

$$T = -2\sqrt{2}ty(x + z) \quad (11a)$$

$$V_{ee} = U(x^2 + z^2) \quad (11b)$$

$$V = \rho \Delta v \quad (11c)$$

with

$$\rho = \langle \Psi | \frac{\hat{n}_1 - \hat{n}_0}{2} | \Psi \rangle = (z^2 - x^2) \quad (12)$$

We call E_0 , E_1 , and E_2 the energies of the ground state, first (singly-)excited state, and second (doubly-)excited state, respectively. These are represented in Fig. 1 as functions of Δv for $t = 1/2$ and $U = 1$. It is worth noting that E_0 (red curve) and E_2 (green curve) are concave and convex with respect to Δv , respectively, for any value of t and U , while E_1 is concave for Δv smaller than a critical value Δv_c (blue curve labeled as E_1^\cap) and becomes convex for $\Delta v > \Delta v_c$ (yellow curve labeled as E_1^\cup).

The corresponding differences in (reduced) site occupation

$$\rho = \frac{\Delta n}{2} \quad (13)$$

for the ground state, ρ_0 , first excited state, ρ_1 , and second excited state, ρ_2 , are represented in Fig. 2. While the ground (red curve) and the doubly-excited (green curve) states have monotonic densities with respect to Δv for any t and U values, ρ_1 is non-monotonic and reaches a critical value ρ_c at Δv_c before decaying to 0 as $\Delta v \rightarrow \infty$. In agreement with Eq. (6b), in the asymmetric Hubbard dimer, one finds

$$\frac{dE_0(\Delta v)}{d\Delta v} = 2\rho_0(\Delta v) \quad (14)$$

However, analogous relations hold true also for the two excited states, i.e.,

$$\frac{dE_1(\Delta v)}{d\Delta v} = 2\rho_1(\Delta v) \quad (15a)$$

$$\frac{dE_2(\Delta v)}{d\Delta v} = 2\rho_2(\Delta v) \quad (15b)$$

Substituting x and z in Eqs. (11a) and (11b) thanks to the normalization condition and the reduced site occupation difference defined in Eqs. (10) and (13), respectively, we obtain the four-branch function

$$f_{\pm\pm}(\rho, y) = -2ty \left(\pm \sqrt{1 - y^2 - \rho} \pm \sqrt{1 - y^2 + \rho} \right) + U(1 - y^2) \quad (16)$$

that one would minimize with respect to y to obtain the exact ground-state functional.^{84,86,87} Although one technically deals with *functions* in the Hubbard dimer, we shall stick to the term *functional* to emphasize the formal analogy between site-occupation function theory and DFT, as customarily done in the literature.^{49,87,90,93-95}

Rather than only minimizing Eq. (16) for a given ρ , we seek *all* stationary points⁶⁷ of $f_{\pm\pm}(\rho, y)$ with respect to y , i.e.,

$$F(\rho) = \text{stat}_y[f_{\pm\pm}(\rho, y)] \quad (17)$$

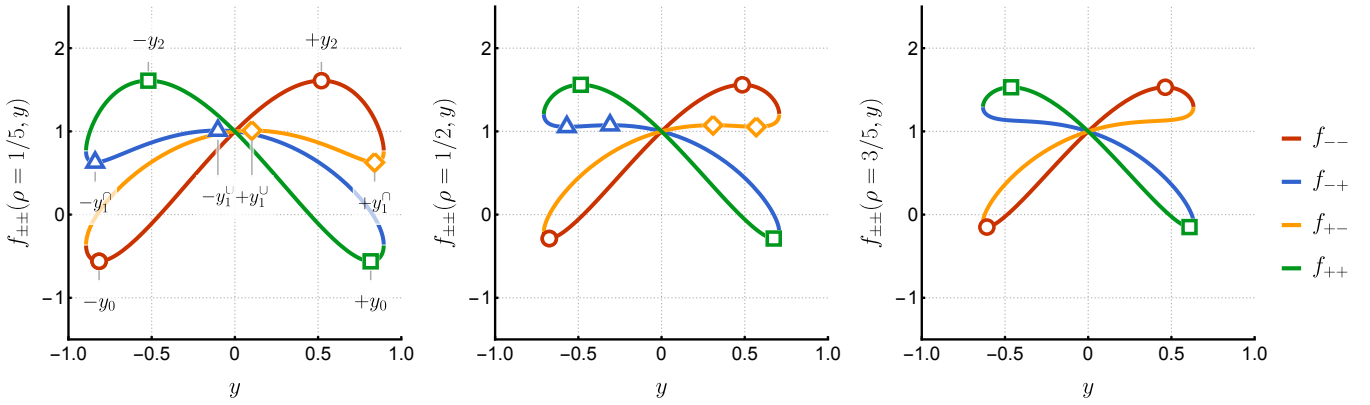


FIG. 3. $f_{--}(\rho, y)$ (red), $f_{-+}(\rho, y)$ (blue), $f_{+-}(\rho, y)$ (yellow), and $f_{++}(\rho, y)$ (green) as functions of y for $t = 1/2$, $U = 1$, and $\rho = 1/5$ (left), $1/2$ (center), and $3/5$ (right). The markers indicate the position of the stationary points on each branch. At $\rho = 3/5$ (right panel), the stationary points of f_{-+} and f_{+-} have disappeared as $\rho > \rho_c$ (see Fig. 2).

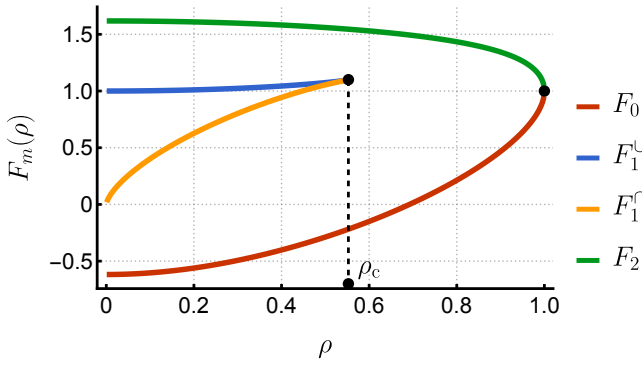


FIG. 4. State-specific exact functionals $F_m(\rho)$ as functions of ρ for $t = 1/2$ and $U = 1$. The ground-state functional $F_0(\rho)$ (red) is convex with respect to ρ , the singly-excited state multi-valued functional $F_1(\rho)$ has one convex branch (blue) and one concave branch (yellow), each associated with a separate set of Δv values, while the doubly-excited state functional $F_2(\rho)$ (green) is concave. Note that F is an even function of ρ .

The choice of the variable over which to optimize in Eq. (17) is arbitrary and several choices are possible yielding various functions⁸⁶ other than $f_{\pm\pm}$, yet identical $F(\rho)$'s. A similar procedure can be carried out via an ensemble formalism,^{22–24} as shown by Fromager and coworkers.^{31–33}

Because, taken as whole, $f_{\pm\pm}$ is symmetric with respect to a change in sign of y , we restrict the discussion to the domain where $y \geq 0$, without loss of generality. As shown in Fig. 3, the branches f_{++} and f_{--} have one stationary point each for $y \geq 0$ (green square and red circle, respectively): the global minimum located at y_0 corresponds to the convex ground-state functional, $F_0(\rho) = f_{++}(\rho, y_0)$, while the global maximum at y_2 corresponds to the concave doubly-excited-state functional, *i.e.*, $F_2(\rho) = f_{--}(\rho, y_2)$ (see Fig. 4). $F_0(\rho)$ and $F_2(\rho)$ merge at $\rho = 1$. The stationary points located at $-y_0$

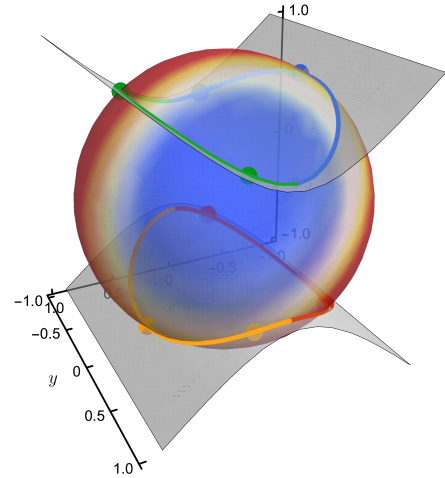


FIG. 5. Illustration of the Levy constrained-search procedure for $t = 1/2$, $U = 1$, and $\rho = 1/5$. The value of $T + V_{ee}$ is mapped on the surface of the unit sphere that represents the normalized wave functions. The gray parabolas correspond to densities $\rho = z^2 - x^2$. The four branches of $f_{\pm\pm}$ [see Eq. (16)] are represented as contours and correspond to the intersections of these three-dimensional objects. The dots locate the stationary points on each of these contours.

and $-y_2$ are associated with opposite values of Δv .

For $\rho < \rho_c$, the branch f_{+-} has two stationary points (yellow diamonds): a local minimum at y_1^\cap and a local maximum at y_1^\cup that yield a concave branch $F_1^\cap(\rho) = f_{+-}(\rho, y_1^\cap)$ (yellow curve in Fig. 4) and a convex branch $F_1^\cup(\rho) = f_{+-}(\rho, y_1^\cup)$ (blue curve in Fig. 4) for the singly-excited-state functional. As expected though, $F_1^\cup(\rho)$ and $F_1^\cap(\rho)$ lead to convex and concave energies, E_1^\cup and E_1^\cap (see Fig. 1), respectively, preserving the property that the energy and the functional are conjugate functions.⁸⁰ Because the density-potential mapping associated with the first excited state is non-invertible (since, as seen in Fig. 2, the same density ρ can be produced by two Δv

values), its “functional” is a partial (*i.e.*, defined for a subdomain of ρ), multi-valued function constituted of one concave and one convex branch that correspond to two separate domains of the external potential. Again, the stationary points on f_{-+} located at $-y_1^\square$ and $-y_1^\cup$ (blue triangles) are associated with opposite values of Δv . At $\rho = \rho_c$, y_1^\square and y_1^\cup merge and disappear for larger ρ values. This critical value of the density decreases with respect to U to reach zero at $U = 0$, and $\rho_c \rightarrow 1$ as $U \rightarrow \infty$.

In accordance with Eq. (6a), the derivative of $F_0(\rho)$ with respect to ρ gives back Δv_0 as a function of ρ , *i.e.*, the inverse of $\rho_0(\Delta v)$ plotted in Fig. 2. Most notably, an analogous relation holds for the excited states. For the doubly-excited state, we simply have

$$\frac{dF_2(\rho)}{d\rho} = -\Delta v_2(\rho) \quad (18)$$

In particular, for $\rho = 0$, we have $\Delta v_2 = 0$, while $\Delta v_2 \rightarrow \infty$ as $\rho \rightarrow 1$, similarly to Δv_0 (except that $\Delta v_0 \rightarrow -\infty$ as $\rho \rightarrow 1$).

For the first-excited state, which has a non-invertible density, $\rho_1(\Delta v)$ (see Fig. 2), we still have

$$\frac{dF_1^\cup(\rho)}{d\rho} = -\Delta v_1^\cup(\rho) \quad (19a)$$

$$\frac{dF_1^\square(\rho)}{d\rho} = -\Delta v_1^\square(\rho) \quad (19b)$$

where $\Delta v_1^\cup(\rho)$ ranges from $-\Delta v_c$ (at $\rho = \rho_c$) to 0^- (for $\rho \rightarrow 0^+$), yielding the inverse of the blue curve in Fig. 2, and $\Delta v_1^\square(\rho)$ ranges from $-\infty$ (for $\rho \rightarrow 0^+$) to $-\Delta v_c$ (for $\rho = \rho_c$), yielding the inverse of the yellow curve in Fig. 2.

The Levy constrained-search procedure is geometrically illustrated in Fig. 5. The surface of the unit sphere corresponds to the normalized wave functions such that $x^2 + y^2 + z^2 = 1$, onto which we have mapped the value of $T + V_{ee}$ as a function of x , y , and z . The gray parabolas correspond to the (potentially unnormalized) wave functions yielding $\rho = z^2 - x^2$. Hence, the contours obtained by the intersection of these three-dimensional surfaces are the normalized wave functions yielding $\rho = z^2 - x^2$. On these contours, one is looking for the points where $f_{\pm\pm}$ is stationary. These are represented by the colored dots in Fig. 5 (see also Fig. 3).

The exact functionals represented in Fig. 4 can also be obtained using the Lieb variational principle. To do so, let us define, for each singlet state, the function

$$f_m(\rho, \Delta v) = E_m - \Delta v \rho \quad (20)$$

However, instead of maximizing the previous expression for a given ρ as in Eq. (5), we seek its entire set of stationary points with respect to Δv for each m value, *i.e.*

$$F_m(\rho) = \text{stat}_{\Delta v}[f_m(\rho, \Delta v)] \quad (21)$$

Figure 6 shows f_m as a function of Δv at $\rho = 0$ and $\pm 1/2$ for each state and the location of the corresponding

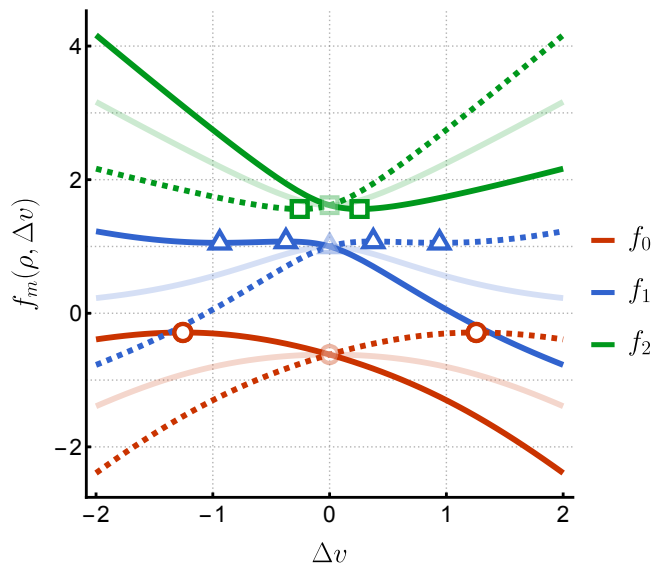


FIG. 6. $f_m(\rho, \Delta v)$ as a function of Δv for $t = 1/2$, $U = 1$, and $\rho = \pm 1/2$: ground state ($m = 0$), singly-excited state ($m = 1$), and doubly-excited state ($m = 2$). The markers indicate the position of the stationary points. The transparent curves correspond to $\rho = 0$. In this case, the linear term $-\Delta v \rho$ in Eq. (5) vanishes and the energy E_m is recovered (see Fig. 1). For $\rho = 1/2$ (solid curves), the linear term shifts the maxima of E_0 and E_1 (red circle and blue triangle, respectively) towards $\Delta v < 0$ and the minimum of E_2 (green square) towards $\Delta v > 0$. Moreover, a local minimum in f_1 (outermost blue triangle) appears. The situation is exactly mirrored for $\rho = -1/2$ (dashed curves).

stationary points. For $\rho = 0$ (transparent curves), one recovers the energies E_m plotted in Fig. 1. The values of the functions f_m at their stationary points (red circle, blue triangle, and green square at $\Delta v = 0$) correspond to the initial values of F_0 , F_1^\cup , and F_2 in Fig. 4. For $\rho = 1/2$, f_0 (solid red curve) and f_2 (solid green curve) have a single extremum: a maximum and a minimum yielding the ground- and second-excited-state functionals, $F_0(\rho)$ and $F_2(\rho)$, respectively, as depicted in Fig. 4. The blue curve f_1 exhibits a local maximum and minimum that correspond to the two branches of the multi-valued functional associated with the first-excited state, $F_1^\square(\rho)$ and $F_1^\cup(\rho)$, respectively.

In practice, Lieb’s formulation has a very neat geometric illustration in the Hubbard dimer. The total energies E_m are “tipped” by the addition of the linear term $-\Delta v \rho$, which shifts their extrema: the maxima of E_0 and E_1 towards $\Delta v < 0$ and the minimum of E_2 towards $\Delta v > 0$. Moreover, in the case of the first-excited state, the linear curve $-\Delta v \rho$ shifts the energy in such a way that, as soon as $\rho > 0$, a local minimum appears (outermost blue triangle) in f_1 . This minimum and the maximum gradually get closer as ρ increases, until they merge at $\rho = \rho_c$, f_1 becoming monotonic with no stationary points for $\rho > \rho_c$. The situation is exactly mirrored for $\rho = -1/2$ (dashed curves).

The present Letter reports the exact functional for the ground and (singlet) excited states of the asymmetric Hubbard dimer at half-filling. To the best of our knowledge, this is the first time that exact function(al)s corresponding to singlet (non-degenerate) excited states are computed. While the ground-state functional is well-known to be a convex function with respect to the site-occupation difference, the functional associated with the highest doubly-excited state is found to be concave. Additionally, and more importantly, we find that the “functional” for the first-excited state is a partial, multi-valued function of the density that is constructed from one concave and one convex branch associated with two separate domains of the external potential. Finally, Levy’s constrained search and Lieb’s convex formulation are found to be entirely consistent with one another, yielding the same exact functionals [Eqs. (17) and (21)] and, even more remarkably, the duality properties of the ground state appear to be shared by the excited states of this model. These findings may provide insight into the challenges of constructing state-specific excited-state density functionals for general applications in electronic structure theory.

This project has received funding from the European Research Council (ERC) under the European Union’s Horizon 2020 research and innovation programme (Grant agreement No. 863481).

- ¹P. Hohenberg and W. Kohn, *Phys. Rev.* **136**, B864 (1964).
- ²A. M. Teale, T. Helgaker, A. Savin, C. Adamo, B. Aradi, A. V. Arbuznikov, P. W. Ayers, E. J. Baerends, V. Barone, P. Calaminici, E. Cancès, E. A. Carter, P. K. Chattaraj, H. Chermette, I. Ciofini, T. D. Crawford, F. De Proft, J. F. Dobson, C. Draxl, T. Frauenheim, E. Fromager, P. Fuentealba, L. Gagliardi, G. Galli, J. Gao, P. Geerlings, N. Gidopoulos, P. M. W. Gill, P. Gori-Giorgi, A. Görling, T. Gould, S. Grimme, O. Gritsenko, H. J. A. Jensen, E. R. Johnson, R. O. Jones, M. Kaupp, A. M. Köster, L. Kronik, A. I. Krylov, S. Kvaal, A. Laestadius, M. Levy, M. Lewin, S. Liu, P.-F. Loos, N. T. Maitra, F. Neese, J. P. Perdew, K. Pernal, P. Pernot, P. Piecuch, E. Rebolini, L. Reining, P. Romaniello, A. Ruzsinszky, D. R. Salahub, M. Scheffler, P. Schwerdtfeger, V. N. Staroverov, J. Sun, E. Tellgren, D. J. Tozer, S. B. Trickey, C. A. Ullrich, A. Vela, G. Vignale, T. A. Wesolowski, X. Xu, and W. Yang, *Phys. Chem. Chem. Phys.* **24**, 28700 (2022).
- ³O. Gunnarsson and B. I. Lundqvist, *Phys. Rev. B* **13**, 4274 (1976).
- ⁴T. Ziegler, A. Rauk, and E. J. Baerends, *Theor. Chem. Acc.* **43**, 261 (1977).
- ⁵O. Gunnarsson, M. Jonson, and B. Lundqvist, *Phys. Rev. B* **20**, 3136 (1979).
- ⁶U. von Barth, *Phys. Rev. A* **20**, 1693 (1979).
- ⁷H. Englisch, H. Fieseler, and A. Haufe, *Phys. Rev. A* **37**, 4570 (1988).
- ⁸E. Runge and E. K. U. Gross, *Phys. Rev. Lett.* **52**, 997 (1984).
- ⁹H. Appel, E. K. Gross, and K. Burke, *Phys. Rev. Lett.* **90**, 043005 (2003).
- ¹⁰K. Burke, J. Werschnik, and E. K. U. Gross, *J. Chem. Phys.* **123**, 062206 (2005).
- ¹¹M. Casida and M. Huix-Rotllant, *Annu. Rev. Phys. Chem.* **63**, 287 (2012).
- ¹²M. Huix-Rotllant, N. Ferré, and M. Barbatti, “Time-dependent density functional theory,” in *Quantum Chemistry and Dynamics of Excited States* (John Wiley & Sons, Ltd, 2020) Chap. 2, pp. 13–46.
- ¹³W. Kohn and L. J. Sham, *Phys. Rev.* **140**, A1133 (1965).
- ¹⁴D. Jacquemin, V. Wathelet, E. A. Perpète, and C. Adamo, *J. Chem. Theory Comput.* **5**, 2420 (2009).
- ¹⁵D. J. Tozer, R. D. Amos, N. C. Handy, B. O. Roos, and L. Serrano-Andres, *Mol. Phys.* **97**, 859 (1999).
- ¹⁶D. J. Tozer and N. C. Handy, *Phys. Chem. Chem. Phys.* **2**, 2117 (2000).
- ¹⁷A. Dreuw, J. L. Weisman, and M. Head-Gordon, *J. Chem. Phys.* **119**, 2943 (2003).
- ¹⁸N. T. Maitra, R. J. C. F. Zhang, and K. Burke, *J. Chem. Phys.* **120**, 5932 (2004).
- ¹⁹B. G. Levine, C. Ko, J. Quenneville, and T. J. Martinez, *Mol. Phys.* **104**, 1039 (2006).
- ²⁰N. T. Maitra, *J. Phys. Cond. Matt.* **29**, 423001 (2017).
- ²¹A. K. Theophilou, *J. Phys. C* **12**, 5419 (1979).
- ²²E. K. U. Gross, L. N. Oliveira, and W. Kohn, *Phys. Rev. A* **37**, 2805 (1988).
- ²³E. K. U. Gross, L. N. Oliveira, and W. Kohn, *Phys. Rev. A* **37**, 2809 (1988).
- ²⁴L. N. Oliveira, E. K. U. Gross, and W. Kohn, *Phys. Rev. A* **37**, 2821 (1988).
- ²⁵A. Pribram-Jones, Z.-h. Yang, J. R. Trail, K. Burke, R. J. Needs, and C. A. Ullrich, *J. Chem. Phys.* **140**, 18A541 (2014).
- ²⁶Z.-H. Yang, J. R. Trail, A. Pribram-Jones, K. Burke, R. J. Needs, and C. A. Ullrich, *Phys. Rev. A* **90**, 042501 (2014).
- ²⁷Z.-H. Yang, A. Pribram-Jones, K. Burke, and C. A. Ullrich, *Phys. Rev. Lett.* **119**, 033003 (2017).
- ²⁸F. Sagredo and K. Burke, *J. Chem. Phys.* **149**, 134103 (2018).
- ²⁹M. Filatov, “Ensemble DFT Approach to Excited States of Strongly Correlated Molecular Systems,” in *Density-Functional Methods for Excited States*, edited by N. Ferré, M. Filatov, and M. Huix-Rotllant (Springer International Publishing, Cham, 2016) pp. 97–124.
- ³⁰B. Senjean, S. Knecht, H. J. A. Jensen, and E. Fromager, *Phys. Rev. A* **92**, 012518 (2015).
- ³¹K. Deur, L. Mazouin, and E. Fromager, *Phys. Rev. B* **95**, 035120 (2017).
- ³²K. Deur, L. Mazouin, B. Senjean, and E. Fromager, *Eur. Phys. J. B* **91**, 162 (2018).
- ³³K. Deur and E. Fromager, *J. Chem. Phys.* **150**, 094106 (2019).
- ³⁴C. Marut, B. Senjean, E. Fromager, and P.-F. Loos, *Faraday Discuss.* **224**, 402 (2020).
- ³⁵P.-F. Loos and E. Fromager, *J. Chem. Phys.* **152**, 214101 (2020).
- ³⁶E. Fromager, *Phys. Rev. Lett.* **124**, 243001 (2020).
- ³⁷F. Cernatic, B. Senjean, V. Robert, and E. Fromager, *Top. Curr. Chem.* **380**, 1 (2022).
- ³⁸T. Gould and S. Pittalis, *Phys. Rev. Lett.* **119**, 243001 (2017).
- ³⁹T. Gould, L. Kronik, and S. Pittalis, *J. Chem. Phys.* **148**, 174101 (2018).
- ⁴⁰T. Gould and S. Pittalis, *Phys. Rev. Lett.* **123**, 016401 (2019).
- ⁴¹T. Gould, G. Stefanucci, and S. Pittalis, *Phys. Rev. Lett.* **125**, 233001 (2020).
- ⁴²T. Gould, L. Kronik, and S. Pittalis, *Phys. Rev. A* **104**, 022803 (2021).
- ⁴³T. Gould, Z. Hashimi, L. Kronik, and S. G. Dale, *J. Phys. Chem. Lett.* **13**, 2452 (2022).
- ⁴⁴T. Gould, D. P. Kooi, P. Gori-Giorgi, and S. Pittalis, *Phys. Rev. Lett.* **130**, 106401 (2023).
- ⁴⁵C. Schilling and S. Pittalis, *Phys. Rev. Lett.* **127**, 023001 (2021).
- ⁴⁶J. Liebert, F. Castillo, J.-P. Labbé, and C. Schilling, *J. Chem. Theory Comput.* **18**, 124 (2021).
- ⁴⁷J. Liebert and C. Schilling, *New J. Phys.* **25**, 013009 (2022).
- ⁴⁸J. Liebert and C. Schilling, *SciPost Phys.* **14**, 120 (2023).
- ⁴⁹J. Liebert, A. Y. Chaou, and C. Schilling, *J. Chem. Phys.* **158**, 214108 (2023).
- ⁵⁰J. P. Perdew and M. Levy, *Phys. Rev. B* **31**, 6264 (1985).
- ⁵¹T. Kowalczyk, T. Tsuchimochi, P.-T. Chen, L. Top, and T. Van Voorhis, *J. Chem. Phys.* **138**, 164101 (2013).
- ⁵²A. T. Gilbert, N. A. Besley, and P. M. Gill, *J. Phys. Chem. A* **112**, 13164 (2008).
- ⁵³G. M. J. Barca, A. T. B. Gilbert, and P. M. W. Gill, *J. Chem. Theory Comput.* **14**, 1501 (2018).
- ⁵⁴G. M. J. Barca, A. T. B. Gilbert, and P. M. W. Gill, *J. Chem.*

- Theory. Comput. **14**, 9 (2018).
- ⁵⁵D. Hait and M. Head-Gordon, *J. Chem. Theory Comput.* **16**, 1699 (2020).
- ⁵⁶D. Hait and M. Head-Gordon, *J. Phys. Chem. Lett.* **12**, 4517 (2021).
- ⁵⁷J. A. R. Shea and E. Neuscamman, *J. Chem. Phys.* **149**, 081101 (2018).
- ⁵⁸J. A. R. Shea, E. Gwin, and E. Neuscamman, *J. Chem. Theory Comput.* **16**, 1526 (2020).
- ⁵⁹T. S. Hardikar and E. Neuscamman, *J. Chem. Phys.* **153**, 164108 (2020).
- ⁶⁰G. Levi, A. V. Ivanov, and H. Jónsson, *J. Chem. Theory Comput.* **16**, 6968 (2020).
- ⁶¹K. Carter-Fenk and J. M. Herbert, *J. Chem. Theory Comput.* **16**, 5067 (2020).
- ⁶²D. Toffoli, M. Quarin, G. Fronzoni, and M. Stener, *J. Phys. Chem. A* **126**, 7137 (2022).
- ⁶³Y. L. A. Schmerwitz, G. Levi, and H. Jónsson, *J. Chem. Theory Comput.* **19**, 3634 (2023).
- ⁶⁴A. Görling, *Phys. Rev. A* **54**, 3912 (1996).
- ⁶⁵A. Nagy, *Int. J. Quantum Chem.* **69**, 247 (1998).
- ⁶⁶M. Levy and A. Nagy, *Phys. Rev. Lett.* **83**, 4361 (1999).
- ⁶⁷A. Görling, *Phys. Rev. A* **59**, 3359 (1999).
- ⁶⁸F. Zhang and K. Burke, *Phys. Rev. A* **69**, 052510 (2004).
- ⁶⁹P. W. Ayers and M. Levy, *Phys. Rev. A* **80**, 012508 (2009).
- ⁷⁰P. W. Ayers, M. Levy, and A. Nagy, *Phys. Rev. A* **85**, 042518 (2012).
- ⁷¹P. W. Ayers, M. Levy, and Á. Nagy, *J. Chem. Phys.* **143**, 191101 (2015).
- ⁷²P. W. Ayers, M. Levy, and A. Nagy, *Theor. Chem. Acc.*, 137 (2018).
- ⁷³L. Garrigue, *Arch. Rational Mech. Anal.* **245**, 949 (2022).
- ⁷⁴E. H. Lieb, in *Density Functional Methods in Physics*, edited by R. M. Dreizler and J. da Providencia (Plenum, New York, 1985) pp. 31–80.
- ⁷⁵R. Gaudoin and K. Burke, *Phys. Rev. Lett.* **93**, 173001 (2004).
- ⁷⁶P. Samal and M. K. Harbola, *J. Phys. B At. Mol. Opt. Phys.* **38**, 3765 (2005).
- ⁷⁷P. Samal, M. K. Harbola, and A. Holas, *Chem. Phys. Lett.* **419**, 217 (2006).
- ⁷⁸E. H. Lieb, *Int. J. Quantum Chem.* **24**, 243 (1983).
- ⁷⁹M. Levy, *Proc. Natl. Acad. Sci. U.S.A.* **76**, 6062 (1979).
- ⁸⁰T. Helgaker and A. M. Teale, in *The Physics and Mathematics of Elliott Lieb* (EMS Press, 2022) pp. 527–559.
- ⁸¹S. Kvaal, U. Ekström, A. M. Teale, and T. Helgaker, *J. Chem. Phys.* **140**, 18A518 (2014).
- ⁸²J. Hubbard, *Proc. Math. Phys. Eng.* **276**, 238 (1963).
- ⁸³E. H. Lieb and F. Wu, *Phys. Rev. Lett.* **20**, 1445 (1968).
- ⁸⁴K. Schonhammer and O. Gunnarsson, *J. Phys. C* **20**, 3675 (1987).
- ⁸⁵A. Montorsi, *The Hubbard Model: A Reprint Volume* (World Scientific, 1992).
- ⁸⁶D. J. Carrascal, J. Ferrer, J. C. Smith, and K. Burke, *J. Phys. Condens. Matter* **27**, 393001 (2015).
- ⁸⁷A. J. Cohen and P. Mori-Sánchez, *Phys. Rev. A* **93**, 042511 (2016).
- ⁸⁸Z.-J. Ying, V. Brosco, G. M. Lopez, D. Varsano, P. Gori-Giorgi, and J. Lorenzana, *Phys. Rev. B* **94**, 075154 (2016).
- ⁸⁹J. C. Smith, A. Pribram-Jones, and K. Burke, *Phys. Rev. B* **93**, 245131 (2016).
- ⁹⁰B. Senjean, M. Tsuchiizu, V. Robert, and E. Fromager, *Mol. Phys.* **115**, 48 (2017).
- ⁹¹D. J. Carrascal, J. Ferrer, N. Maitra, and K. Burke, *Eur. Phys. J. B* **91**, 142 (2018).
- ⁹²M. Penz and R. van Leeuwen, *J. Chem. Phys.* **155**, 244111 (2021).
- ⁹³K. Capelle and V. L. Campo Jr, *Phys. Rep.* **528**, 91 (2013).
- ⁹⁴T. Dimitrov, H. Appel, J. I. Fuks, and A. Rubio, *New J. Phys.* **18**, 083004 (2016).
- ⁹⁵S. Giarrusso and A. Pribram-Jones, *J. Chem. Phys.* **157**, 054102 (2022).